Magnetic Frustration, Phase Competition, and the Magnetoelectric Effect in $NdFe_3(BO_3)_4$

J. E. Hamann-Borrero,[1,*] S. Partzsch,[1] S. Valencia,[2] C. Mazzoli,[3,4] J. Herrero-Martin,[5,4] R. Feyerherm,[2] E. Dudzik,[2] C. Hess,[1] A. Vasiliev,[6] L. Bezmaternykh,[7] B. Büchner,[1,8] and J. Geck[1]

[1]*Leibniz Institute for Solid State and Materials Research, IFW-Dresden, 01171 Dresden, Germany*
[2]*Helmholtz Zentrum Berlin, Albert Einstein Straße 15, 12489 Berlin, Germany*
[3]*Politecnico di Milano e unità CNISM, piazza Leonardo Da Vinci 32, I-20133 Milano, Italy*
[4]*European Synchrotron Radiation Facility (ESRF), BP 220, 38043 Grenoble, France*
[5]*Institut de Ciència de Materials de Barcelona, ICMAB-CSIC, Campus Universitari de Bellaterra, E-08193 Bellaterra, Barcelona, Spain*
[6]*Low Temperature Physics department, Faculty of Physics, Moscow State University, Moscow 119992, Russia*
[7]*L.V Kirensky Institute of Physics, Siberian Division, Russian Academy of Sciences, Krasnoyarsk 660036, Russia*
[8]*Institute for Solid State Physics, Technische Universität Dresden, 01062 Dresden, Germany*

(Received 30 July 2012; published 26 December 2012)

We present an element selective resonant magnetic x-ray scattering study of $NdFe_3(BO_3)_4$ as a function of temperature and applied magnetic field. Our measurements show that the magnetic order of the Nd sublattice is induced by the Fe spin order. When a magnetic field is applied parallel to the hexagonal basal plane, the helicoidal spin order is suppressed and a collinear ordering, where the moments are forced to align in a direction perpendicular to the applied magnetic field, is stabilized. This result excludes a noncollinear spin order as the origin of the magnetically induced electric polarization in this compound. Instead our data imply that magnetic frustration results in a phase competition, which is the origin of the magnetoelectric response.

DOI: 10.1103/PhysRevLett.109.267202 PACS numbers: 75.85.+t, 75.25.−j, 75.30.Et, 78.70.Ck

The coupling between magnetism and electric polarization in so-called multiferroic materials is a major topic of current condensed matter research, since it is of large interest for both basic science and technological applications [1,2]. Unfortunately ferroelectric and magnetic order rarely coexist and even if they do, the coupling between them is usually very weak [2].

It was therefore greeted with great excitement when frustrated magnetic materials were discovered, where the coupling of magnetic and ferroelectric orders is extraordinarily strong. Typically these systems relieve the magnetic frustration to some extent via, e.g., lattice distortions, which, as a byproduct, also create a ferroelectric polarization [1–3]. In this way the magnetic and ferroelectic (FE) orders are directly connected to one another, resulting in a very strong magnetoelectric coupling.

Typical examples are noncollinear magnets [4], where the spin order rotates about an axis $\mathbf{e}$ and propagates along a given direction $\mathbf{q}$. In these magnetic phases a FE polarization $\mathbf{P}$ can exist, which, according to the conventional theory, is given by $\mathbf{P} \propto \mathbf{e} \times \mathbf{q}$ [4,5]. However, there is another mechanism where FE order can be driven by collinear spin order [1,6]. In order to determine what the microscopic origin of the magnetoelectric (ME) coupling really is, it is therefore very important to know the type of magnetic order.

Among multiferroic systems that show noncollinear spin order, the ME $NdFe_3(BO_3)_4$ has attracted considerable attention due to the large coupling between magnetic and electric orders [7,8]. Upon cooling in zero magnetic field, a collinear magnetic order sets in first at $T_N \approx 30$ K, consisting of ferromagnetic hexagonal ab planes, which are stacked antiferromagnetically along the perpendicular c direction (cf. Fig. 1) [9,10]. Recent polarized neutron scattering experiments [10] have shown that a commensurate (C) to incommensurate (IC) transition is present at $T_{IC} \approx 13.5$ K. At this temperature the magnetic structure turns into an IC spin helix that propagates along the c axis. Although this neutron study revealed important details about the helical spin order in $NdFe_3(BO_3)_4$, the microscopic origin of the spin helix remains to be clarified.

Even more interesting, at low temperatures, the electric polarization strongly increases when a magnetic field is applied parallel to a, reaching a maximum of $P_a \sim 390\ \mu C/m^2$ at $B_a \sim 1.3$ T and 4.5 K [7,11] (in $TbMnO_3$ $P_c \sim 800\ \mu C/m^2$ [3]). The spin helix in zero field cannot explain the electric polarization since $\mathbf{e} \parallel \mathbf{q}$, for which the conventional theory yields $\mathbf{P} = 0$. This already implies that the spin order in applied magnetic fields must change. As stated already above, it is essential to determine these changes in order to uncover the driving force behind the ME coupling. To date, however, the spin order in applied magnetic fields is unknown for this compound.

In this Letter we clarify the two central questions mentioned above, namely the origin of the spin helix as well as the magnetic order in applied magnetic fields. By means of resonant magnetic x-ray scattering (RMXS) we show that the magnetic order of the Nd sublattice is induced by the Fe-spin order and determine the magnetic field induced changes in the spin order. The obtained data provide clear

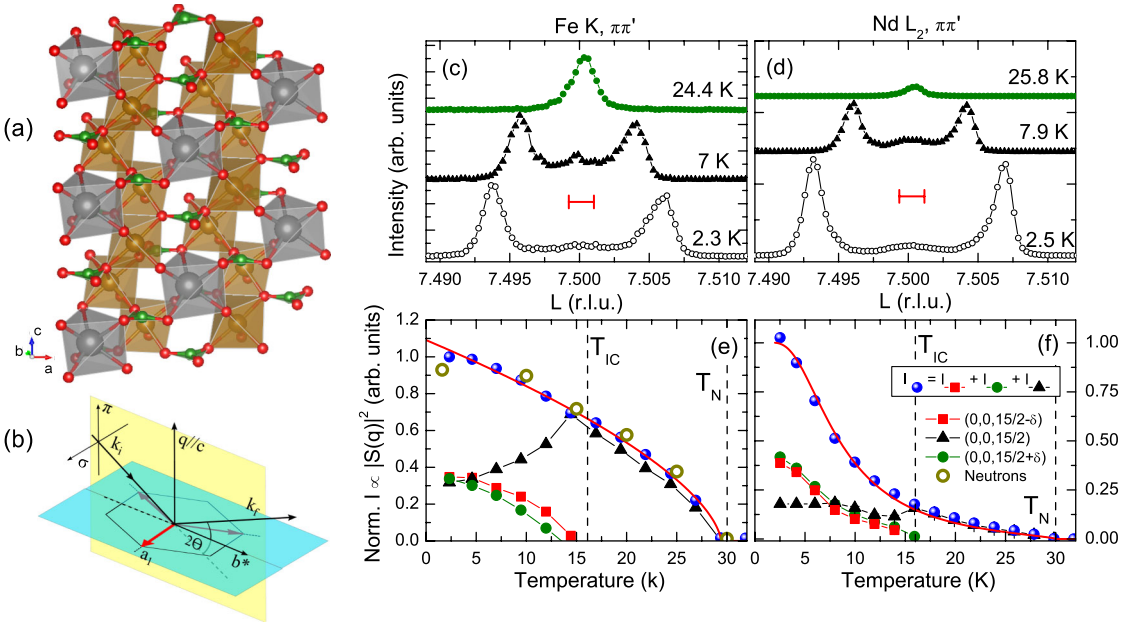

FIG. 1 (color online). (a) Crystal structure of $NdFe_3(BO_3)_4$ with Fe chains of octahedra (brown), Nd prisms (gray) and the B triangles (green). (b) Experimental scattering geometry showing the scattering plane (yellow, light gray) and the hexagonal basal plane (blue, dark gray) where the a axis is perpendicular to the scattering plane. Temperature dependent intensities of the magnetic (0, 0, 15/2) reflection at the Fe K (c) and Nd L_2 (d) edges. The corresponding normalized integrated intensities are given in panels (e) and (f). Open circles in (e) show the T-dependent Fe moment, squared and scaled for comparison, from neutron diffraction (taken from Ref. [9]). Red scales in (c) and (d) show the (0, 0, 6) Bragg peak FWHM = 0.0018(3) r.l.u. Thick red lines are fits to the data as explained in the text.

experimental evidence that the C-IC transition and the ME effect are both related to the magnetic frustration between the Nd and the Fe sublattice.

RMXS measurements at the Nd L_2 (6.726 keV) and Fe K (7.128 keV) edges were performed at beam lines ID20 (ESRF in Grenoble, France [12]) and MagS (BESSY, Berlin [13]). A scheme of the scattering geometry used for the present experiments is illustrated in Fig. 1(b). The sample was mounted inside a cryomagnet with the horizontal scattering plane parallel to the b^*c plane of the sample. Measurements down to 2 K and with magnetic fields up to 2 T along the crystallographic a axis were performed; i.e., the magnetic field was aligned perpendicular to the scattering plane. During the measurements both the incoming and the outgoing photon polarizations were controlled, where σ (σ') and π (π') refer to linearly incoming (outgoing) polarized light perpendicular and parallel to the scattering plane, respectively.

$NdFe_3(BO_3)_4$ crystallizes in a hexagonal structure with space group $R32$ with the hexagonal unit cell parameters $a \approx 9.59$ Å, $c \approx 7.61$ Å [9]. As shown in Fig. 1(a), the structure consists of chains of edge shared FeO_6 octahedra along the crystallographic c axis. These chains are connected by BO_3 triangles and NdO_6 prisms. $NdFe_3(BO_3)_4$ therefore hosts two coupled magnetic sublattices of, respectively, Fe and Nd sites.

Below $T_N \sim 30$ K, the appearance of superlattice reflections at $\mathbf{q} = (0, 0, 3l \pm \frac{3}{2})$ (where l is an integer) reveals a doubling of the unit cell along c [see Figs. 1(c) and 1(d)]. This observation is in perfect agreement with recent neutron [9,10] as well as x-ray scattering [14] reports. The simultaneous appearance of these reflections together with the magnetic order and the fact that the reflected photons for incoming π polarization are mostly σ polarized, clearly identifies these reflections as magnetic superlattice peaks.

Figures 1(c) and 1(d) show high-resolution scans of the (0, 0, 15/2) magnetic reflection at different temperatures, which were measured at the Fe K and Nd L_2 edge, respectively for $B = 0$ T. Below $T_N \approx 30$ K a single C reflection (green circles) is observed, corresponding to the collinear AFM structure [9,10,14]. Upon further cooling down to $T_{IC} \approx 16$ K the peak splits into two IC peaks at (0, 0, $15/2 \pm \delta$) due to the formation of a long period spin helix (black triangles) that propagates along the c direction [9,10]. Surprisingly, although the C reflection becomes very weak and broad, it never vanishes completely which indicates a coexistence of the C and IC phases at $T < T_{IC}$.

The value of δ strongly increases below T_{IC} as does the intensity of the IC reflections (open circles). This temperature dependent δ reveals a continuous change of the helix periodicity. Specifically, we find that, in real space, the period of the spin helix decreases from ~3900 Å (~523 unit cells) at 14 K to ~1123 Å (~146 unit cells) at 2 K. Again, these observations are in very good agreement with previous neutron results [10].

Within the kinematical theory of magnetic diffraction, the RMXS integrated intensity at the Fe K and the Nd L_2 edge is directly related to the ordered magnetic moment on the Fe and the Nd sublattice, respectively [15,16]. In other words, RMXS enables us to study the magnetic order on the Fe and Nd sublattices separately by tuning the photon energy to the corresponding absorption edge.

Figure 1(e) shows the temperature dependent integrated RMXS intensities measured at the Fe K edge and normalized to its value at the lowest temperature. As can be observed in this figure, the C peak first increases rapidly with cooling below T_N. Upon further cooling below T_{IC}, the C reflection collapses whereas the IC reflections appear and increase in intensity.

A similar peak splitting behavior is also observed at the Nd L_2 edge. However, here the temperature evolution of the intensities is very different. As shown in Fig. 1(f), the intensity enhancement of the C peak is much weaker in the range $T_{IC} < T < T_N$. Below T_{IC} the C peak intensity barely changes, while the IC peaks' intensities increase pronouncedly.

The blue circles in Figs. 1(e) and 1(f) correspond to the total integrated intensity obtained by adding the intensities of the C and the IC peaks. This total integrated intensity is proportional to $\langle S_{Fe}\rangle^2$ at the Fe K and $\langle S_{Nd}\rangle^2$ at the Nd L_2 edge, where $\langle S_{Fe}\rangle$ and $\langle S_{Nd}\rangle$ denote the magnetic order parameter for the Fe and the Nd sublattice, respectively.

The measured $\langle S_{Fe}\rangle^2$ displays the typical behavior expected for a magnetic ordering transition and compares well to the corresponding neutron diffraction results [open circles in Fig. 1(e)].

$\langle S_{Nd}\rangle^2$ exhibits a completely different temperature dependence and, in particular, does not show a clear phase transition at T_N. To understand the magnetic ordering behavior of the Nd sublattice, the corresponding curve in Fig. 1(f) was fitted to a mean field model, which assumes that the Nd order is merely induced by the Fe ordering [17]:

$$|S_{Nd}|^2 = \left[S^o_{Nd} \tanh\left(\frac{S^o_{Nd} \lambda_{Fe\text{-}Nd} 6 \langle S_{Fe}\rangle}{2 k_B T} \right) \right]^2. \quad (1)$$

In this equation k_B is the Boltzmann constant, $\lambda_{Fe\text{-}Nd}$ is the effective Fe-Nd coupling constant, S^o_{Nd} is the Nd ordered moment at $T = 0$ K. Further, we used $\langle S_{Fe}\rangle^2 = [S^o_{Fe}(1 - T/T_N)^\beta]^2$ as a parameterization, where $S^o_{Fe} = 5/2$ is the ordered Fe moment at $T = 0$ and $\beta = 0.31(2)$ was determined by a fit to the experimental data [red line in Fig. 1(e)]. The factor 6 accounts for the number of nearest Fe neighbors around each Nd in the crystal. Note that $\lambda_{Fe\text{-}Nd}\langle S_{Fe}\rangle$ is the magnetic mean field due to the Fe neighbors of the Nd sites that induces the magnetic order on the Nd sublattice.

The red solid line in Fig. 1(f) shows the fit of Eq. (1) to the experimental data. The best fit is obtained using $S^o_{Nd} = 2.7 \mu_B$ determined from neutron diffraction [9] and $\lambda_{Fe\text{-}Nd} = 0.30(1)\ T/\mu_B$ [18]. The excellent agreement with the data implies that the magnetic order on the Nd sublattice is induced by the driving Fe spin order.

The intensity maps shown in Fig. 2 display the temperature dependence of the magnetic (0, 0, 15/2) reflection measured at the Nd L_2 edge in different applied magnetic fields. According to the previous neutron scattering studies, the magnetic moments of both Nd and Fe are always confined to the hexagonal ab plane [9,10]. In this situation, the point symmetry of the Nd sites implies (cf. Ref. [21]) that the RMXS of the Nd sites can be described using the formulae given in Refs. [22,23]; i.e., the intensities $I_{\pi\pi'}$ and $I_{\pi\sigma'}$ can be expressed as: $I_{\pi\pi'} \propto (z_a \sin 2\theta)^2$ and $I_{\pi\sigma'} \propto (-z_{b^*} \cos\theta)^2$, where θ is the scattering angle and z_n are the projections of the magnetic moments along the crystallographic a and b^* directions [cf. Fig. 1(b)].

As can be seen in Figs. 2(a) and 2(b) no qualitative difference between the two intensities is observed for $B = 0$ T apart from the fact that $I_{\pi\pi'}/I_{\pi\sigma'} \sim 3$. The relative intensities in the two scattering channels are the result of a particular domain structure. For instance, in the C phase the magnetic moments of the various domains are aligned along 3 equivalent directions within the hexagonal ab plane [Fig. 2(g)]. This yields $z_a, z_{b^*} \neq 0$ and intensities in both the $\pi\pi'$ and the $\pi\sigma'$ channel, where the value of

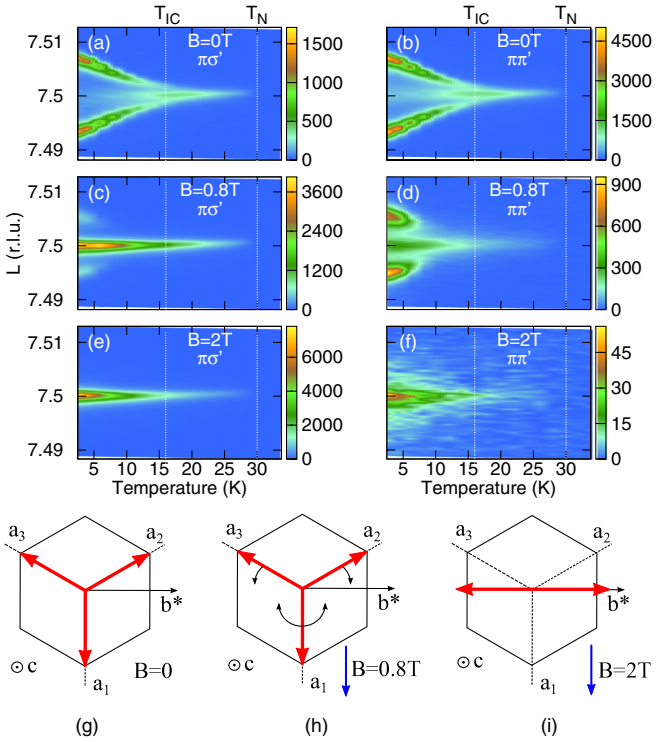

FIG. 2 (color online). Temperature dependence of the (0, 0, 15/2) peak in different applied magnetic fields. $\pi\sigma'$ and $\pi\pi'$ scattering is shown in the left and right panels, respectively. The magnetic field was always applied parallel to the a axis. Color boxes at the right of the figures indicate the intensity in arb. units. (g), (h), (i): Illustration of the spin directions as a function of magnetic field. Red arrows correspond to the easy axes of different magnetic domains in the c phase.

$I_{\pi\pi'}/I_{\pi\sigma'}$ depends on the volume fractions occupied by the different domains in the probed volume.

More importantly, there are already remarkable changes in the RMXS for $B = 0.8$ T [Figs. 2(c) and 2(d)]. First, the IC phase is suppressed and only observed at lower temperatures. Second, there is an overall intensity transfer from $\pi\pi'$ to $\pi\sigma'$. This implies a reduction of z_a and an increase of z_{b^*}; i.e., the spins in the different domains rotate as illustrated in Fig. 2(h). This observation agrees with magnetization [14,24] and sound velocity [25] measurements which show that at $B = 0.8$ T the system is in the center of a hysteresis corresponding to a spin flop transition.

When increasing the magnetic field to $B = 2$ T, the IC phase is completely suppressed, as can be seen in Figs. 2(e) and 2(f). In this field, pure $\pi\sigma'$ scattering is observed, whereas the $\pi\pi'$ is very weak, amounting only to 0.5% of the $\pi\sigma'$ intensity. This implies that $z_a = 0$, which means that the spin moments are now essentially perpendicular to **B**, i.e., parallel to b^* [Fig. 2(i)]. Note also that the intensity in Fig. 2(e) is equal to the sum of the intensities measured in Figs. 2(a) and 2(b) showing that at $B = 2$ T a single collinear magnetic domain is formed.

These field dependent measurements reveal that the maximum of magnetic field induced ferroelectric polarization **P** coexists with collinear spin order. The spin helix and any noncollinear order can hence be excluded as an origin for the magnetoelectric effect in $NdFe_3(BO_3)_4$. The presence of magnetic domains influences the transition from the spin helix phase in zero field to the field-induced collinear phase; i.e., the domains determine how the system switches between the non-FE and the FE phase. These effects will be subject of a forthcoming publication. In the following, however, we will focus on the microscopic effects inside a single domain only.

The microscopic insights obtained by RMXS enable us to deduce a consistent scenario for the magnetoelectric coupling in $NdFe_3(BO_3)_4$, which is based on the magnetic frustration between the Fe and Nd sublattices: according to previous reports [9], Fe has a $3d^5$ configuration, which implies that both the Fe-Fe and the Nd-Fe superexchange interactions are antiferromagnetic (AFM). Our data further show that $\langle S_{\mathrm{Fe}}\rangle^2$ corresponds to the primary order parameter, whereas $\langle S_{\mathrm{Nd}}\rangle^2$ is merely induced. We therefore consider the coupling of Nd to fully ordered Fe chains. As illustrated in Fig. 3, the AFM Nd-Fe interactions are frustrated, even though not all Nd-Fe couplings have the same strength. Upon decreasing temperature $\langle S_{\mathrm{Nd}}\rangle^2$ increases; i.e., an average magnetic moment on the Nd sites develops. This finite $\langle S_{\mathrm{Nd}}\rangle^2$ then also increases the energy related to the Nd-Fe frustration in the collinear phase.

Without applied magnetic field, this Nd-Fe frustration can be relieved by forming a spin helix, which optimizes the magnetic interactions and gains exchange energy ΔE_{IC} by slight rotations $\Delta\phi$ of neighboring spins along c.

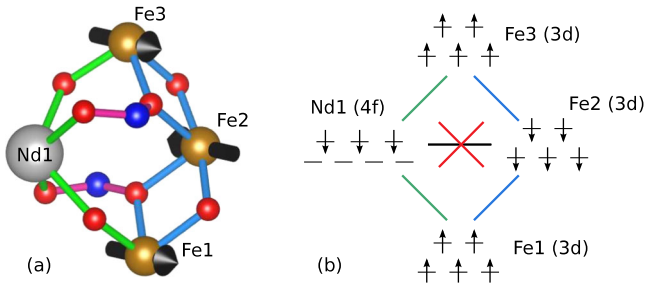

FIG. 3 (color online). (a) Crystal structure of $NdFe_3(BO_3)_4$ showing the next nearest neighbor superexchange paths between Fe-Fe (blue, dark gray) and Nd-Fe (green, light gray). Only one of the three equivalent Fe-chains surrounding Nd is shown. (b) Magnetic frustration between Nd1 and Fe2 ions. The strongest coupling is given by the intra chain Fe-Fe AFM coupling. The Fe1,3-Nd1 and Fe2-Nd1 are expected to be weaker.

Since $\langle S_{\mathrm{Nd}}\rangle^2$ increases upon cooling, $\Delta E_{\mathrm{IC}}/\Delta\phi$ will also depend on temperature, which naturally explains the strongly temperature dependent period $\lambda \propto 1/\Delta\phi$ of the spin helix. We therefore conclude that the spin helix is driven by the Nd-Fe sublattice frustration.

By applying a magnetic field parallel to the ab plane, the spin helix is rapidly suppressed and the spin rotations are no longer energetically favorable. We propose that within the magnetic field enforced C phase, the system chooses an alternative way to relieve the magnetic frustration, which involves a modulation of the lattice structure and creates a FE polarization. We cannot determine these distortions based on the present data, but the threefold rotation axis of the space group $R32$ has to be broken in order to allow for a ferroelectric polarization parallel to the ab plane. Interestingly, this removes the symmetry relations exactly between the Fe sites shown in Fig. 3(a) [26]. The required symmetry reduction is therefore fully consistent with the deduced microscopic mechanism, which further supports our conclusions.

$NdFe_3(BO_3)_4$ hence belongs to a class of materials where the magnetoelectric properties are driven by the magnetic frustration of two interacting subsystems and where the degree of frustration can even be tuned by changing temperature. This frustration can be relieved either by forming a spin helix or by creating a FE polarization. The FE collinear and the non-FE spin helix are therefore competing phases. Due to this competition an external magnetic field can easily switch between the two phases, causing the ME effect. We believe that a quantitative theoretical analysis of this mechanism may help to identify new magnetoelectric materials with optimized properties. The presented RMXS study also beautifully illustrates the power of this experimental technique and shows how this enables us to unveil hidden microscopic physics that can hardly be accessed otherwise. This strongly motivates further studies of materials with different interacting magnetic sublattices using RMXS.

The authors would like to thank C. Detlefs and J. Trinckauf for fruitful discussions. For technical support during the experiments we would like to thank H. Walker and the ESRF and BESSY for beam time provision. This work was supported by the DFG through the Emmy Noether Programme (Grant No. GE1647/2-1) and the European Community's Seventh Framework Program (FP7/2007-2013) under Grant No. 226716.

*j.e.hamann.borrero@ifw-dresden.de

[1] S.-W. Cheong and M. Mostovoy, Nat. Mater. **6**, 13 (2007).
[2] D. Khomskii, Physics **2**, 20 (2009).
[3] T. Kimura, T. Goto, H. Shintani, K. Ishizaka, T. Arima, and Y. Tokura, Nature (London) **426**, 55 (2003).
[4] M. Mostovoy, Phys. Rev. Lett. **96**, 067601 (2006).
[5] Y. Tokura and S. Seki, Adv. Mater. **22**, 1554 (2010).
[6] Y. J. Choi, H. T. Yi, S. Lee, Q. Huang, V. Kiryukhin, and S. W. Cheong, Phys. Rev. Lett. **100**, 047601 (2008).
[7] A. K. Zvezdin, G. P. Vorobev, A. M. Kadomtseva, Y. F. Popov, A. P. Pyatakov, L. N. Bezmaternykh, A. V. Kuvardin, and E. Popova, JETP Lett. **83**, 509 (2006).
[8] A. M. Kadomtseva, A. K. Zvezdin, A. P. Pyatakov, A. V. Kuvardin, G. P. Vorobev, Y. F. Popov, and L. N. Bezmaternykh, JETP **105**, 116 (2007).
[9] P. Fischer, V. Pomjakushin, D. Sheptyakov, L. Keller, M. Janoschek, B. Roessli, J. Schefer, G. Petrakovskii, L. Bezmaternikh, V. Temerov, and D. Velikanov, J. Phys. Condens. Matter **18**, 7975 (2006).
[10] M. Janoschek, P. Fischer, J. Schefer, B. Roessli, V. Pomjakushin, M. Meven, V. Petricek, G. Petrakovskii, and L. Bezmaternikh, Phys. Rev. B **81**, 094429 (2010).
[11] A. M. Kadomtseva, Y. F. Popov, G. P. Vorobev, A. P. Pyatakov, S. S. Krotov, K. I. Kamilov, V. Y. Ivanov, A. A. Mukhin, A. K. Zvezdin, A. M. Kuzmenko, L. N. Bezmaternykh, I. A. Gudim, and V. L. Temerov, Low Temp. Phys. **36**, 511 (2010).
[12] L. Paolasini, C. Detlefs, C. Mazzoli, S. Wilkins, P. P. Deen, A. Bombardi, N. Kernavanois, F. de Bergevin, F. Yakhou, J. P. Valade, I. Breslavetz, A. Fondacaro, G. Pepellin, and P. Bernard, J. Synchrotron Radiat. **14**, 301 (2007).
[13] E. Dudzik, R. Feyerherm, W. Diete, R. Signorato, and C. Zilkens, J. Synchrotron Radiat. **13**, 421 (2006).
[14] J. E. Hamann-Borrero, M. Philipp, O. Kataeva, M. v. Zimmermann, J. Geck, R. Klingeler, A. Vasiliev, L. Bezmaternykh, B. Büchner, and C. Hess, Phys. Rev. B **82**, 094411 (2010).
[15] M. Blume and D. Gibbs, Phys. Rev. B **37**, 1779 (1988).
[16] D. Gibbs, D. R. Harshman, E. D. Isaacs, D. B. McWhan, D. Mills, and C. Vettier, Phys. Rev. Lett. **61**, 1241 (1988).
[17] M. N. Popova, S. A. Klimin, E. P. Chukalina, E. A. Romanov, B. Z. Malkin, E. Antic-Fidancev, B. V. Mill, and G. Dhalenne, Phys. Rev. B **71**, 024414 (2005).
[18] Due to different definitions of the mean field, the values of λ_{fd} in Refs. [19,20] are related to our value by $\lambda_{fd} = 2\lambda_{\text{Fe-Nd}}$.
[19] E. A. Popova, D. V. Volkov, A. N. Vasiliev, A. A. Demidov, N. P. Kolmakova, I. A. Gudim, L. N. Bezmaternykh, N. Tristan, Y. Skourski, B. Büchner, C. Hess, and R. Klingeler, Phys. Rev. B **75**, 224413 (2007).
[20] E. A. Popova, N. I. Leonyuk, M. N. Popova, E. P. Chukalina, K. N. Boldyrev, N. Tristan, R. Klingeler, and B. Büchner, Phys. Rev. B **76**, 054446 (2007).
[21] M. W. Haverkort, N. Hollmann, I. P. Krug, and A. Tanaka, Phys. Rev. B **82**, 094403 (2010).
[22] J. P. Hannon, G. T. Trammell, M. Blume, and D. Gibbs, Phys. Rev. Lett. **61**, 1245 (1988).
[23] J. P. Hill and D. F. McMorrow, Acta Crystallogr. Sect. A **52**, 236 (1996).
[24] D. V. Volkov, A. A. Demidov, and N. P. Kolmakova, JETP **104**, 897 (2007).
[25] G. Zvyagina, K. Zhekov, I. Bilych, A. Zvyagin, I. Gudim, and V. Temerov, Low Temp. Phys. **37**, 1269 (2011).
[26] The maximal nonisomorphic subgroup that allows such symmetry reduction is $C2$, corresponding to a monoclinic setting. For instance, Fe1, Fe2, and Fe3 in Fig. 3(a) are symmetry related in the $R32$ space group but they are not in $C2$. Thus atomic displacements of these ions (or ligand ions attached to them) might induce some electric polarization parallel to the ab plane.